View metadata, citation and similar papers at core.ac.uk

brought to you by CORE

provided by Elsevier - Publisher Connector

Developmental Biology 333 (2009) 297–311

Contents lists available at ScienceDirect

Developmental Biology

journal homepage: www.elsevier.com/developmentalbiology

Late extraembryonic morphogenesis and its zen^{RNAi}-induced failure in the milkweed bug *Oncopeltus fasciatus*

Kristen A. Panfilio *

University Museum of Zoology, Department of Zoology, Downing Street, Cambridge CB2 3EJ, UK
Institute for Developmental Biology, University of Cologne, Gyrhofstraβe 17, 50931 Cologne, Germany

ARTICLE INFO

Article history:
Received for publication 9 April 2009
Revised 23 June 2009
Accepted 27 June 2009
Available online 4 July 2009

Keywords:
Insect extraembryonic membranes
Epithelial morphogenesis
Biomechanics
zen (*zerknüllt*)
Oncopeltus fasciatus
Katatrepsis
Serosa
Amnion

ABSTRACT

Many insects undergo katatrepsis, essential reorganization by the extraembryonic membranes that repositions the embryo. Knockdown of the *zen* gene by RNA interference (RNAi) prevents katatrepsis in the milkweed bug *Oncopeltus fasciatus*. However, the precise morphogenetic defect has been uncertain, and katatrepsis itself has not been characterized in detail. The dynamics of wild type and zen^{RNAi} eggs were analyzed from time-lapse movies, supplemented by analysis of fixed specimens. These investigations identify three zen^{RNAi} defects. First, a reduced degree of tissue contraction implies a role for *zen* in baseline compression prior to katatrepsis. Subsequently, a characteristic 'bouncing' activity commences, leading to the initiation of katatrepsis in wild type eggs. The second zen^{RNAi} defect is a delay in this activity, suggesting that a temporal window of opportunity is missed after *zen* knockdown. Ultimately, the extraembryonic membranes fail to rupture in zen^{RNAi} eggs: the third defect. Nevertheless, the outer serosal membrane manages to contract, albeit in an aberrant fashion with additional phenotypic consequences for the embryo. These data identify a novel epithelial morphogenetic event – rupture of the 'serosal window' structure – as the ultimate site of defect. Overall, *Oncopeltus zen* seems to have a role in coordinating a number of pre-katatreptic events during mid embryogenesis.

© 2009 Elsevier Inc. All rights reserved.

Introduction

Most insect eggs are characterized by two extraembryonic membranes, the amnion and the serosa. These membranes surround the early embryo, with the amnion covering the embryo's ventral surface and the outer serosa enveloping the amnion, embryo, and yolk. However, as *extra*embryonic structures, the membranes are only temporary attributes of the insect egg. In later development they often retreat and uncover the embryo before they degenerate or are discarded at hatching (reviewed in Panfilio, 2008).

Membrane uncovering is essential for successful embryogenesis in many lineages. If it does not occur or occurs only partially, the embryo remains confined by the amnion at the time of embryonic flank outgrowth for dorsal closure. In the confined position, the embryonic flanks are forced to grow within the amniotic cavity and to close over the appendages, resulting in an everted, or inside out, body arrangement that is clearly lethal (Ando, 1955; Erezyilmaz et al., 2004; Liu and Kaufman, 2004; Mori, 1975; Novák, 1969; Panfilio et al., 2006; Sander, 1959; Sander, 1960; Truckenbrodt, 1979; van der Zee et al., 2005). Two recent studies have identified homologues of the *zen* gene, which encodes a derived Hox transcription factor with extraembryonic expression, as essential for accomplishing membrane uncovering in the hemimetabolous milkweed bug *Oncopeltus fasciatus* and in the holometabolous red flour beetle *Tribolium castaneum* (Panfilio et al., 2006; van der Zee et al., 2005). However, these initial characterizations have left ambiguities regarding the precise defect in a complex morphogenetic movement that involves fusion, rupture, and contraction events and requires the coordination of the serosa and amnion. Furthermore, previous research on the *zen* (*zerknüllt*) gene in the fruit fly *Drosophila melanogaster* had identified a fundamentally different role for *zen* in extraembryonic tissue specification in early development (Wakimoto et al., 1984). Thus the investigations of *zen* in the bug and beetle identified a new role in an unexpected and little-studied developmental process. Further exploration of the role of *zen* is therefore an opportunity to better understand the membrane morphogenesis role of this gene and to elucidate the nature of the affected wild type developmental process.

In this study I have pursued characterization of wild type events and of their derailment after RNA interference (RNAi) for the *zen* gene in the bug *Oncopeltus fasciatus*. Like nearly all hemimetabolous insects, *Oncopeltus* has a mode of extraembryonic membrane uncovering that concomitantly repositions the embryo within the egg, an event known as katatrepsis (Panfilio, 2008). Although this is topographically more complex than a simple uncovering event, the fundamental requirements of tissue interaction are the same. Furthermore, knockdown of *Oncopeltus zen* is the only known way of completely blocking this morphogenetic movement; all other perturbations in the studies cited

* Fax: +49 221 470 5164.
E-mail address: kristen.panfilio@alum.swarthmore.edu.

0012-1606/$ – see front matter © 2009 Elsevier Inc. All rights reserved.
doi:10.1016/j.ydbio.2009.06.036

above result in only a partial failure, or in a mixture of full or partial failure across eggs. Thus knockdown of *Oncopeltus zen* (*Of-zen*) provides a uniquely simple tool to study membrane uncovering.

This paper addresses two questions. What is necessary for wild type katatrepsis to occur? Specifically, what are the preceding, preparatory events? Secondly, at what step do *Of-zen*^{RNAi} eggs fail? Are they truly inert due to a serosal defect, as previously characterized (Panfilio et al., 2006)? To address these questions, I have employed two, complementary methodological approaches. The topographical relationship of the serosa, amnion, and embryo are examined with fixed specimens. To gain insight into the dynamics of the system, time-lapse movie data are used.

Materials and methods

Oncopeltus *culture, RNA interference*

O. fasciatus were maintained in laboratory cultures established from the stock at Carolina Biological Supply (Burlington, USA), following the company's husbandry advice. Eggs were collected in intervals of ≤2 h and incubated at 25 °C, 68% relative humidity. Throughout this paper, age is that at the time of collection, or minimum age.

Parental RNA interference was performed as described previously (Panfilio et al., 2006). Double stranded RNA preparations of the 400 bp *Of-zen* molecule "ds iii" were injected into adult females at concentrations of 0.2 μg/μl or 2 μg/μl (5 μl total volume). Negative controls were: 5 μl of injection buffer only, or a 678 bp fragment of the *DsRed* gene (5 μl: 0.2 μg/μl). Throughout this paper, all phenotypically wild type data are from truly wild type eggs from uninjected mothers. However, phenotypically wild type eggs from negative control or *zen*-injected mothers did not differ from true wild type with respect to the timing or duration of examined developmental events (data not shown).

Time-lapse movie set up, acquisition, and analysis

Immediately prior to filming, eggs were selected and positioned on dry glass slides. Selection was based on the clarity of the 'serosal window', which is indicative of incipient katatrepsis stage (see Results). During filming, microscope stage temperature was 24.9 ± 1.4 °C (mean ± range). All embryos were scored at hatching age; there was no difference in embryogenesis between filmed and unfilmed embryos.

Time-lapse movies were recorded with a Zeiss AxioCam MRm camera and Zeiss Axioskop 2 mot plus microscope driven by Zeiss AxioVision (version 4.5) software. Image acquisition was under bright field conditions with air objectives: 5× for whole-egg views, 20× for posterior pole views. With the 5× objective three eggs could be filmed simultaneously, including a control wild type egg alongside *zen*^{RNAi} eggs. Images were acquired every 30 s. Transmitted light illumination was on only during image acquisition. Exposure time was set manually (11–16 ms). Eggs were filmed for 5–22 h. Periodically, filming was stopped for data back up, resulting in brief (≤4.3 min) gaps.

Movies were analyzed with AxioVision software (v. 4.5 or 4.6.3). Distance was measured with digital calipers, between parallel lines demarcating the chorion at the posterior pole and the posteriormost extent of the embryo's head. To eliminate bias, the head line was removed between measurements. To confirm accuracy, in the wild type data set all measurements were made at least twice; values were averaged. Measurements were made at least every 2.5 min. For the *Of-zen*^{RNAi} data set, measurements were made at bounce minima and at the temporal midpoint between minima (adjusted to ensure the midpoint was not during a bounce). Area was measured and structures were outlined with the software's "spline outline" function. Statistical tests are Student's *t*-Tests and Chi-square tests, using the algorithms available at http://www.physics.csbsju.edu/stats/ (site accessed May–September, 2008).

Egg fixation and staining

Most eggs were heat fixed, dechorionated in heptane:methanol, and chemically fixed as previously described (Panfilio et al., 2006). For immunohistochemistry, this method was compared with an alternative to avoid heat fixation and no qualitative difference was found for the antibody used. Some eggs prepared for semithin sectioning were fixed in a third way. Live eggs were submerged in phosphate buffered saline (PBS) and pricked ≥2 times with a fine glass needle to permeablize the chorion. The eggs were then fixed in ice-cold fixative solution (1 part 2.5% glutaraldehyde/PBS, 2 parts 1% osmium tetroxide/PBS) for 1 h. Eggs were then washed 5 min each: 3× PBS, 2× PBS/distilled water (dH_2O), and 2× dH_2O.

For semithin sectioning, eggs were embedded in araldite. The araldite mixture (10 ml Araldite CY212, 10 ml DDSA hardener [dodecenyl succinic anhydride], 0.4 ml BDMA accelerator [benzyldimethlamine]) was made with reagents from Agar Scientific (Stansted, UK), according to the preparation advice in Glauert (1975). Fixed eggs were dehydrated from dH_2O to ethanol (10 min each: 50%, 70%, 90%, 95%, 100% ethanol) and transferred to acetone or transferred directly from storage methanol to acetone (2× 15 min). Eggs were gently rotated overnight in an airtight vial in an acetone 1:1 araldite mixture. The acetone was allowed to evaporate, and eggs were incubated in fresh araldite solution overnight with rotation. Eggs were then positioned in molds within the araldite and polymerized at 70 °C for two days. Resin blocks were cut into 1 or 2 μm sections using a Reichert-Jung Ultracut E microtome and glass knives prepared with an LKB Knifemaker (Type 7801 A, Stockholm). Sections were dried onto a glass slide at 60 °C, stained with methylene blue (2% methylene blue/1% boric acid), washed with tap water, dried, and sealed with DPX mountant (BDH Laboratory Supplies, Poole, UK).

Whole egg topography was visualized by methylene blue or basic fuchsin staining followed by yolk clearing. Eggs were stained with methylene blue solution 1:500 methanol for 15 min, washed briefly in methanol, and then stepped from methanol to BBBA (benzyl benzoate 2:1 benzyl alcohol). Fuchsin staining followed established protocol (Wigand et al., 1998), including mounting in benzyl benzoate 4:1 benzyl alcohol.

To assay for apoptosis, an antibody against the cleaved form of human Caspase-3 (Cell Signaling Technology, Danvers, Massachusetts, USA) was used at 1:40, followed by an anti-rabbit secondary at 1:500 with either an alkaline phosphatase (Roche) or Alexa Fluor 568 (Invitrogen) conjugate. Eggs were washed 3× 5 min in PBS with 0.1% Tween-20 (PBT), incubated for 2–2.5 h at room temperature (RT) in blocking solution (5% normal goat serum/2 mg/ml bovine serum albumin/PBT), then incubated with the primary antibody in fresh blocking solution overnight at 4 °C. Eggs were washed in PBT (2–2.5 h, 4–6 washes) and incubated in blocking solution (2.25–3 h) at RT. Incubation with the secondary antibody in fresh blocking solution was again overnight at 4 °C. Finally eggs were washed in PBT (2–2.75 h, 4–6 washes, RT) and transferred to Vectashield mountant (Vector Laboratories, Burlingame, California, USA). Enzymatic, pigment-based detection followed the protocol established for *in situ* hybridization (Liu and Kaufman, 2004), and samples were stored in 70% glycerol/PBS.

Fluorescent nuclear staining was with YOPRO-1 iodide (1 μM, Invitrogen) with simultaneous RNase treatment (1 μg/ml, Qiagen) in PBT or with TOTO-3 iodide (1 μM, Invitrogen; no RNase treatment). As a single stain, staining was 30–60 min followed by PBT washes (1.25 h, 4–6 washes, RT). For immunohistochemistry, the staining was simultaneous with secondary antibody incubation.

Image processing and manipulation

Images taken on dissecting and compound microscopes were captured with digital cameras driven by commercial software. In some figures, images of different focal depths were manually stacked to

produce a single image. For confocal microscopy, specimens were visualized with a Leica TCS SP1 or SP2 confocal laser-scanning microscope driven by dedicated software (Leica Microsystems, Heidelberg, Germany). Optical sections (every 5 or 10 μm) were compiled into single images using the "maximum projection" mode. Some images were adjusted globally for "levels" in Photoshop (Adobe Systems) so that the range of pixel detection did not exceed the actual range of the image. Some nuclear counterstains were selectively darkened to lessen embryonic relative to extraembryonic signal. Movie files were generated by exporting still images from AxioVision, resizing them in Photoshop, and compiling them into QuickTime (.mov) files with ImageJ (version 1.40 g, NIH) software.

Results

Results are first presented for the wild type characterization, and then for zen^{RNAi} eggs. Katatrepsis is briefly introduced, and then events are presented chronologically. As zen^{RNAi} eggs never undergo katatrepsis itself, preparatory events and subsequent dorsal closure are most germane to the comparison.

Katatrepsis is a backflip movement that maintains continuous tissue over the egg surface

Katatrepsis is the movement by which the embryo is everted from the yolk and extraembryonic membranes, and its axes come to correspond to those of the egg. Prior to this event, the germband stage embryo lies within the egg and is inverted with respect to the anterior–posterior and dorsal–ventral axes of the egg. At the incipient katatrepsis stage, the serosa and amnion are fused in a region at the posterior egg pole, just over the embryo's head (Figs. 1A, F, F′; see below). Katatrepsis initiates when the serosa contracts, rupturing the extraembryonic tissue within the fused area and exposing the embryo. Continued serosal contraction pulls the amnion and embryo out and over the posterior pole. Thus the embryo undergoes a backflip that corrects its formerly inverted position while it progressively emerges:

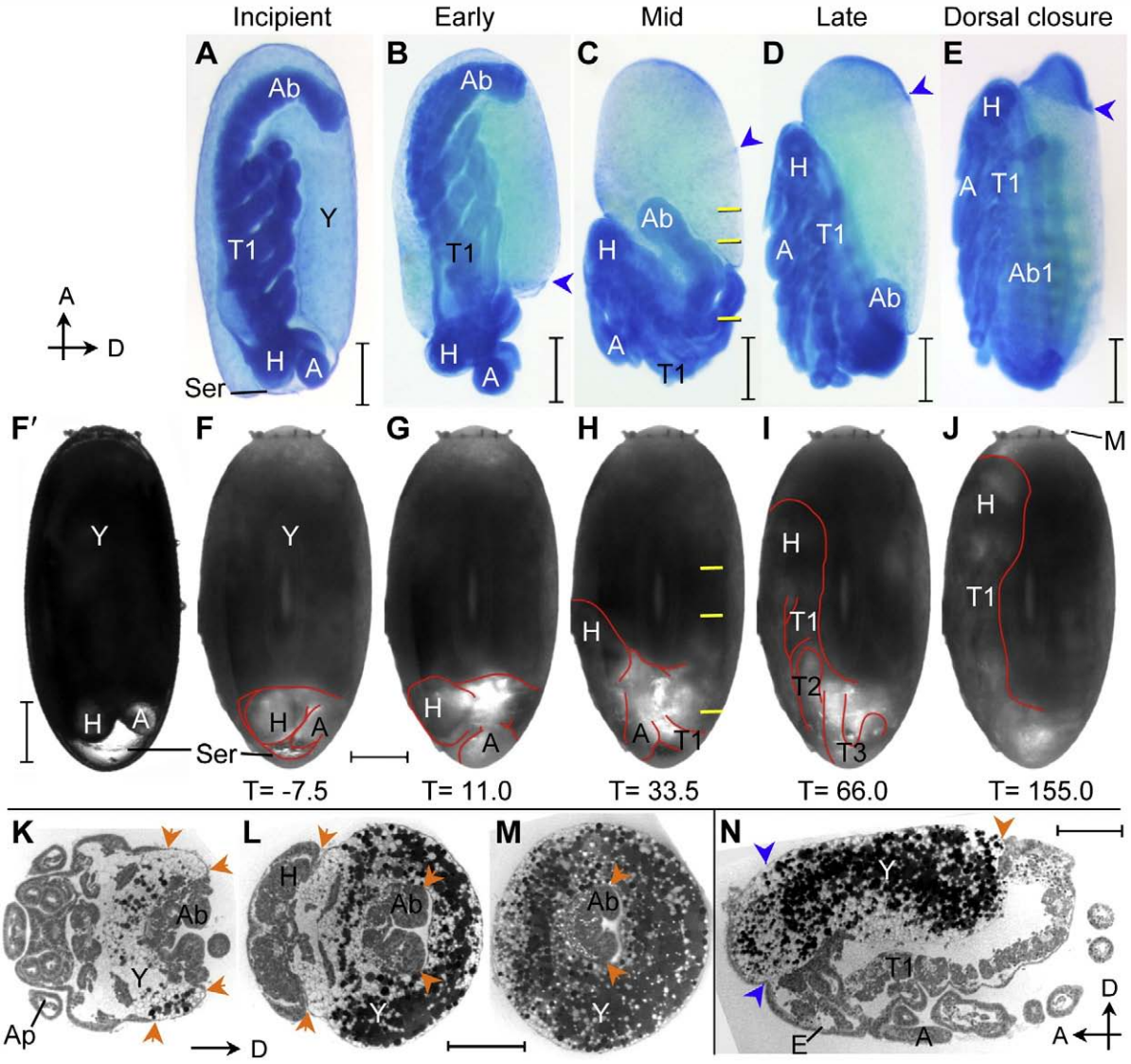

Fig. 1. Progression of *Oncopeltus* katatrepsis illustrated with fixed specimens (A–E), time-lapse movie stills (F–J), and sectioned material (K–N). Images (F–J) are from Movie S1; time in minutes is given relative to the start of katatrepsis. The embryo is inside the chorion and the micropyles mark the anterior pole. The serosa is labeled at the site of amnion–serosa fusion (A, F, F′). Image (F′) is of a live embryo immersed in oil rather than air, enhancing visibility of the serosal window at a comparable stage to (F). (K–M) Progressively more anterior transverse sections through a mid stage egg: approximate locations are indicated by yellow lines in (C, H). Late stage sagittal section (N). Arrowheads indicate tissue borders: orange, amnion–embryo; blue, serosa–amnion. Orientation: (A–J) egg-anterior is up and egg-dorsal is right (views are lateral); (K–M) egg-dorsal is right and the right side is up; (N) egg-anterior is right and egg-dorsal is up. Abbreviations: A, antenna; Ab(1), abdomen/abdominal segment (1); Ap, appendage; E, eye; H, head; M, micropyles; Ser, serosa; T1–3, thoracic segment 1–3; Y, yolk. Scale bars are 200 μm.

first the head and antennae (early stage, Figs. 1B, G), then the legs (mid stage, Figs. 1C, H), and lastly the abdomen (late stage, Figs. 1D, I). Katatrepsis is immediately followed by dorsal closure, during which time the embryo's head fully reaches the anterior egg pole (Figs. 1E, J).

Throughout katatrepsis, the embryo, amnion, and serosa create a continuous sheet of tissue over the egg surface, with the membranes comprising single layered epithelia (Figs. 1K, N: note the continuity of the amnion with the serosa and embryo: arrowheads). This is particularly apparent at mid katatrepsis, when the embryo and amnion are a U-shape of tissue that is half-in/half-out of the yolk (Figs. 1K–M). In particular, the amnion and the serosa remain firmly attached to one another at their common border (Fig. 1, blue arrowheads), which enables contraction by the serosa to reposition the amnion and embryo.

Wild type preparation for katatrepsis involves reorganization of the embryo, amnion, and serosa

Preparation for katatrepsis involves reorganization of the late germband embryo, amnion, and serosa (Fig. 2). Completion of these events heralds the incipient katatrepsis stage.

The extended germband embryo curves back on itself around the anterior egg pole and is roughly 140% egg length (EL; Fig. 2A). During germband retraction (Figs. 2B–C), the body thickens and length is reduced to only slightly more than 100% EL, with a flexed abdomen. Consolidation also includes medial, caudad folding of the appendages, which become tucked close to the ventral epidermis. The exception to this organization is the antennae, whose bulbous distal tips curl out and cephalad.

Changes in the embryo are reflected in a concomitant remodeling of the amnion. During germband stages the amnion is collapsed over the ventral surface of the embryo (Fig. 2A: arrows). The custom fit of the amnion includes individual wrapping of the appendages, which lie in their own pockets of the fluid-filled amniotic cavity (Fig. 2B″). Germband retraction and appendage folding correlate with the smoothing of these pockets into an unbranched cavity, which is consequently expanded up to 5× its previous height over the embryo (*cf.* Figs. 2B, C). After membrane rupture, amniotic cavity volume increases still further, presumably due to the pulling force of the serosa separating amnion from embryo (Fig. 2D).

A second, important pre-katatrepsis change is that the amnion becomes apposed to and fuses with the serosa. Although the embryo's head and amnion never lie very deep below the surface, there is a small quantity of yolk separating the two membranes at germband stages (Figs. 2A′, E). Prior to the completion of germband retraction, the intervening yolk is eliminated and the amnion and serosa together form the 'serosal window' (Fig. 2B′). The term 'serosal window' refers to the round region of extraembryonic covering through which the

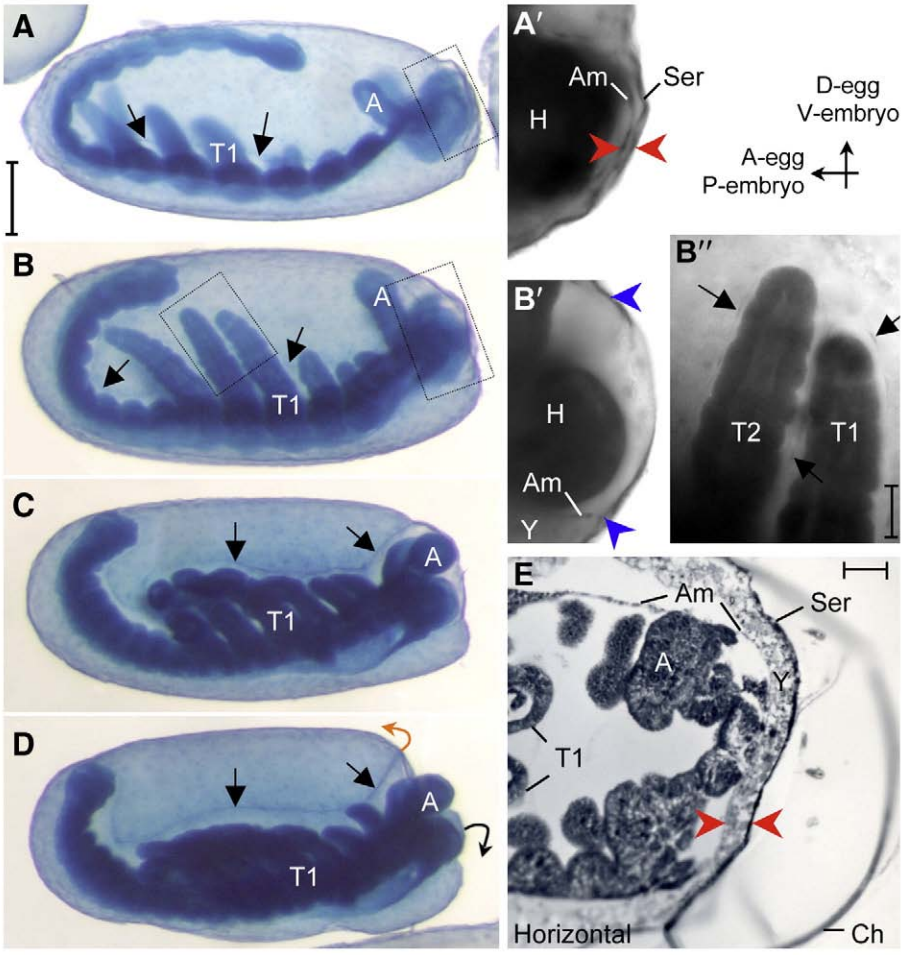

Fig. 2. Wild type (WT) tissue reorganization during: (A) extended germband, (B) retracting germband, (C) incipient katatrepsis, (D) early katatrepsis stages. At germband stages, individual pockets of the amniotic cavity enclose the appendages (B″) and the amnion and serosa are separate (A′, red arrowheads). (E) Semithin sectioning shows the membranes are separated by a thin film of yolk (red arrowheads). Later the membranes fuse, forming the serosal window (B′, blue arrowheads). Black arrows indicate portions of the amnion that are in focus. Colored arrows in (D) indicate the direction of emergence of the amniotic (orange) and embryonic (grey) tissue. In (E), tissue shrinkage away from the chorion is not expected to affect relative topography. Images with the same letter label are of the same egg. Images are lateral, with egg-anterior left and egg-dorsal up, except (E) is a slightly oblique horizontal (frontal) section. Additional abbreviations: Am, amnion; Ch, chorion. Scale bars: 200 μm for A–D; 50 μm for B″ and E. Image (C) is the same as Fig. 1A.

embryo's head is visible at the incipient katatrepsis stage (Cobben, 1968; Mahr, 1960; Schwalm, 1988). This is distinct from the open 'serosal window' at the time of extraembryonic membrane formation in those species that form the membranes from folds (Handel et al., 2000). Just as the early serosal window will be the site of final closure of the developing membranes, the later serosal window (sense used here) will be the site of initial opening of the mature membranes (*cf.* Figs. 2C and D), and in each case the perimeter of the window comprises the amnion-serosa border that delimits the extent of the membranes' connection.

Wild type eggs 'bounce' during the pre-katatrepsis period

In addition to topographical changes, incipient katatrepsis is marked by the onset of new activity (Movie S1). There is a 'bouncing' of the serosal sack (extraembryonic membranes, yolk, embryo, amniotic cavity) that initiates near the anterior egg pole, propagates down the length of the egg, and results in a posteriorward shift of the embryo's head and the serosal window before they return to a resting position. The term bouncing refers to the recurrent back-and-forth movement of the embryo's head, the most visible consequence of this egg activity. Bouncing has been observed in all wild type eggs filmed at this stage ($N=38$). It may initiate any time between 2.2 and 8.8 h prior to membrane rupture (= the initiation of katatrepsis; mean = 5.0 h, standard deviation: $\sigma=2.0$, $N=17$), and include 8–25 individual bounces ($N=6$).

To quantitatively characterize bouncing, I analyzed movies of 5 eggs filmed at higher magnification of the posterior pole region (*e.g.* Movie S2). This data set includes recordings up to 4 h prior to katatrepsis, for a total of 16.5 h sampled at 570 time points, with 45 documented bounces (Fig. 3).

Bouncing is quasi-periodic and frequent. On average, it occurs every 22 min (mean time between bounce minima, $N=40$, $\sigma=7.5$), although time between individual bounces varies substantially (range: 6.4–50.5). An average bounce lasts 8.7 min ($\sigma=2.6$, range: 3.5–16), and during the 4 h prior to katatrepsis an average egg spends 35% of its time bouncing ($\sigma=17$, range: 17–63%).

Bounces are small, gradual movements of the serosal sack, involving a displacement of about 11 μm at 3 μm/min as measured by embryonic head position (see Materials and methods). For context, an *Oncopeltus* egg is generally 1.2 mm long ($N=23$). The posteriorward, initial phase is significantly faster, farther, and takes less time than the anteriorward, return phase (Table 1A–C). Thus a bounce is likely to leave the embryo in a more posterior position than previously ($\chi^2=4.67$, 1 degree of freedom, $P=0.031$), albeit only by 1.6 μm on average. Nonetheless, bouncing does not inevitably shift the embryo posteriorward, as the period between bounces is not static and may be characterized by overall posteriorward or anteriorward shift (Fig. 3, *cf.* e1 and e3 plots). Bounces are often (47%, $N=45$) immediately preceded by a small anteriorward contraction, which enhances the bounce. Bounces that are preceded by a contraction of at least 1 μm are significantly faster and farther on the posteriorward phase than those that are not (Table 1D–E).

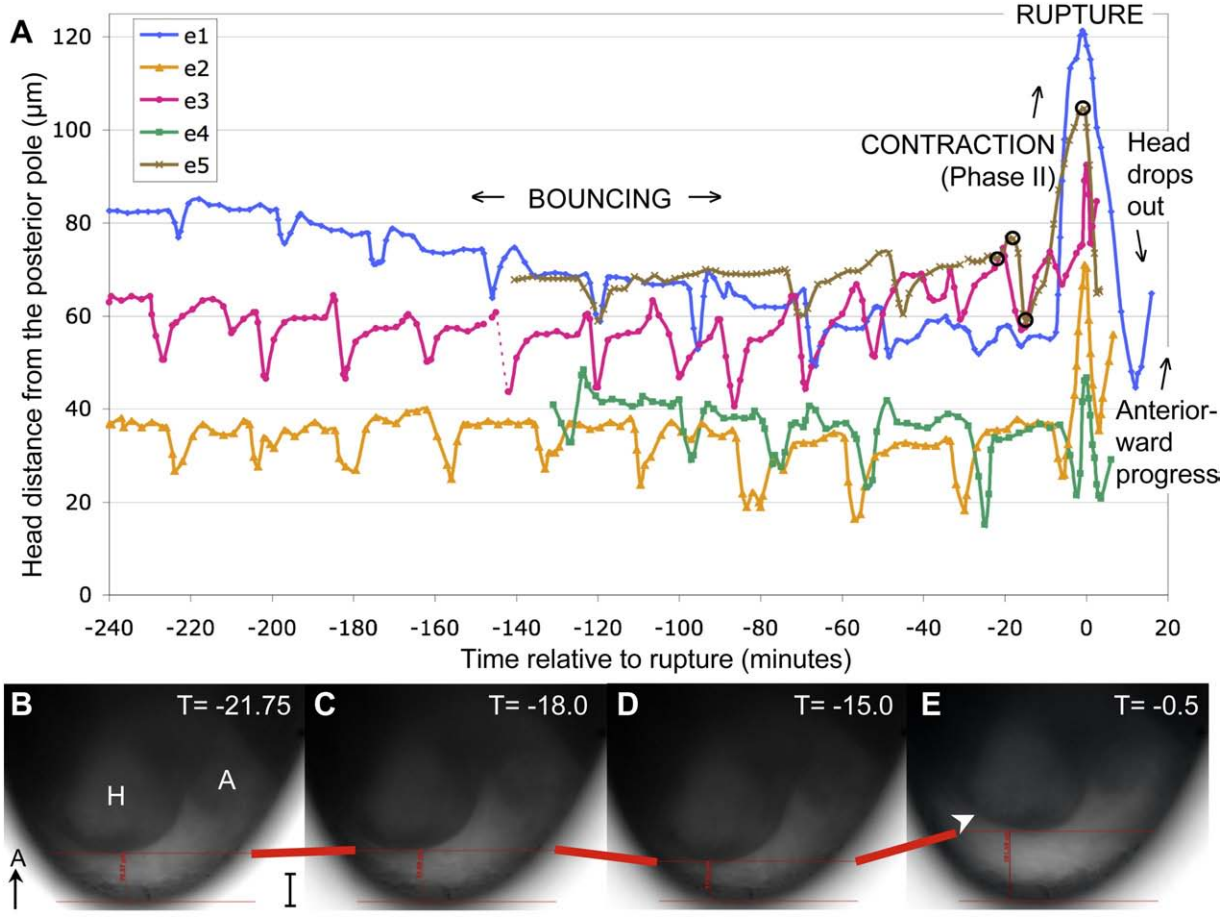

Fig. 3. WT bouncing activity and the initiation of katatrepsis. (A) Distance of the posteriormost position of the top of the embryo's head from the posterior pole of the chorion as a function of time in five eggs (this is a proxy measure for the serosal window and, therefore, the entire serosal sack, as embryonic tissue is more visible). Membrane rupture begins at time 0. Gaps in some plots reflect brief filming pauses (see Materials and methods). (B–E) Still images of egg 5 (time relative to rupture given; black circles in A indicate corresponding plot points), showing the starting point, maxima, and minimum positions during the final bounce and prior to rupture. Thin red lines in the still images show distance measurements (see Materials and methods). Thick red lines across images emphasize change in position. The arrowhead in (E) highlights head deformation during Phase II contraction (see main text for details of Phases I and II). Images are lateral with egg-anterior up and egg-dorsal right. Scale bar is 50 μm.

Table 1
Statistical test values from live imaging data of wild type and *Of-zen*^{RNAi} eggs (see main text for details).

Test ID	*t*-test type	Tested feature	Data set A mean	Data set B mean	*t* value	Degrees of freedom	Probability (*P*)
WT posteriorward (data set A) versus anteriorward (data set B) phases of bounces							
A	Prd	Rate (μm/min)	3.7	2.4	3.90	41	<0.0001**
B	Prd	Time (min)	3.6	5.1	−3.41	41	0.001**
C	Prd	Distance (μm)	12.3	10.7	3.28	41	0.002**
WT bounces with (A) or without (B) a preceding contraction ≥1 μm							
D	Unp	Rate (μm/min)	4.3	3.3	−2.27	36	0.029*
E	Unp	Distance (μm)	15.2	10.0	−4.27	36	<0.0001**
WT average anteriorward bounce phase (A) versus contraction for katatrepsis (B) per embryo							
F	Prd	Rate (μm/min)	2.6	8.3	−4.60	4	0.010**
G	Prd	Distance (μm)	10.6	39.6	−3.00	4	0.040*
WT (A) versus before katatrepsis age (BK) *zen-RNAi* (B) bouncing behavior, serosal window							
H	Unp	Bounce start age (h)	92.72	96.88	−2.14	9	0.061 NS
I	Unp	Bounce duration (min)	7.6	6.3	2.97	119	0.0036**
J	Unp	Bounce frequency (min)	22.4	18.9	3.08	110	0.0026**
K	Unp	Bounce amplitude (μm)	11.9	9.2	1.56	75	0.12 NS
L	Unp	Interbounce position (μm)	81.2	68.1	3.48	77	0.0008**
M	Unp	Window area (%: μm^2 window/ μm^2 egg)	9.52	7.11	9.73	77	<0.0001**
WT or BK *zen-RNAi* (A) versus after katatrepsis age (AK) *zen-RNAi* (B) bouncing behavior							
N	Unp	WT versus AK frequency (min)	22.4	16.4	6.71	188	<0.0001**
O	Unp	BK versus AK frequency (min)	18.9	16.4	2.87	178	0.0046**
P	Unp	BK versus AK amplitude (μm)	9.2	21.3	−6.19	155	<0.0001**
Q	Unp	BK versus AK duration (min)	6.3	7.7	−3.86	177	0.0002**
R	Unp	BK versus AK interbounce position (μm)	68.1	46.2	7.29	155	<0.0001**
S	Unp	WT versus AK bounce minima position (μm)	52.8	24.6	7.95	170	<0.0001**
T	Unp	BK versus AK bounce minima position (μm)	59.4	24.6	10.3	158	<0.0001**
WT (A) or *zen-RNAi* (B) embryo minimum age at the completion of dorsal closure waves							
U	Unp	Minimum age (h)	106.7	107.0	0.176	14	0.86 NS

Abbreviations: min, minute; Prd, paired; Unp, unpaired; WT, wild type; *, $P \leq 0.05$; **, $P \leq 0.01$; NS, not significant.

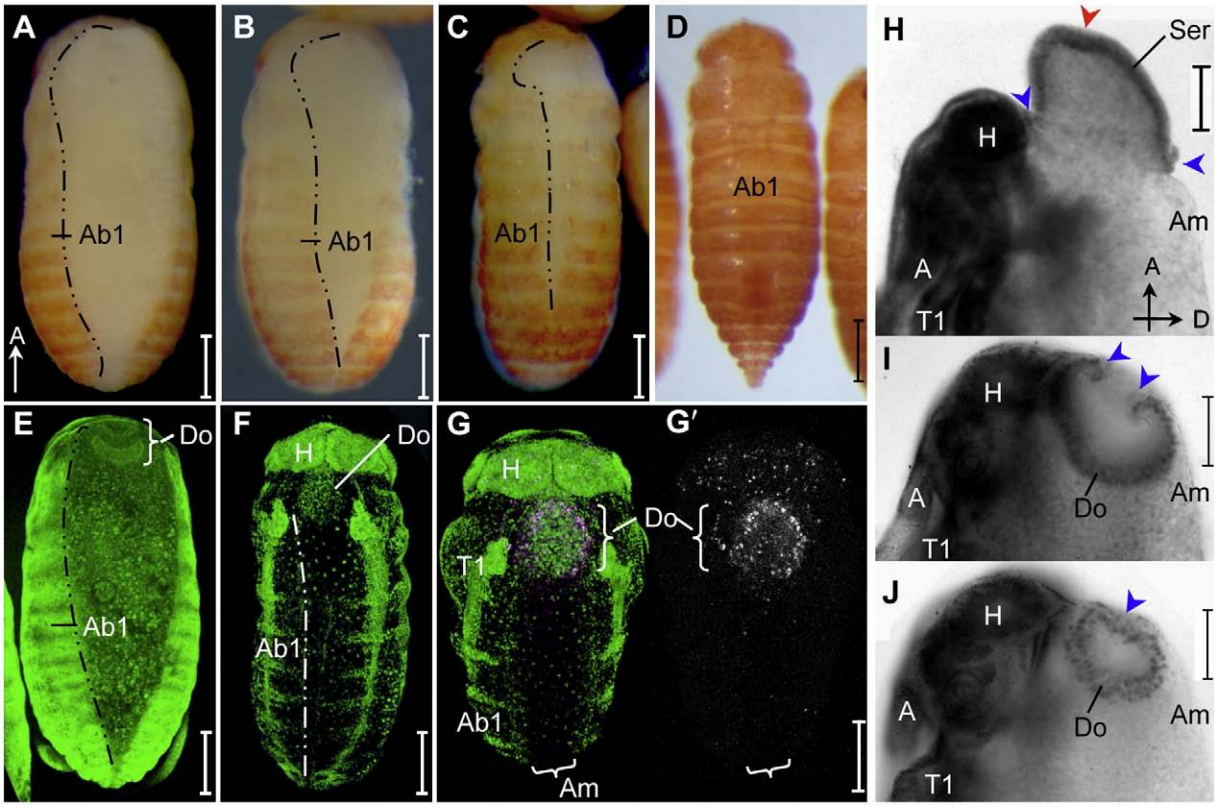

Fig. 4. WT dorsal closure, and apoptosis of the serosa. (A–D) Light micrographs show the posterior-to-anterior progression of dorsal closure and the darkening of pigmentation. (E–F) Confocal projections show the discoidal shape of the dorsal organ (= contracted serosa) at two time points (autofluorescence and nuclear stain, respectively). Dotted lines indicate the position of the embryonic flank (left side only). (G) During late dorsal closure, the serosa dies by apoptosis (magenta: Caspase-3; green: nuclear counterstain). Apoptosis can also be seen in neural sculpting of the brain lobes. (H–J) Late serosal reorganization from an anterior cap (*cf.* Fig. 1E) to the dorsal organ involves invagination (red arrowhead) and curling up of the serosal edges (blue arrowheads). Images are in dorsal (A–F), dorsal-anterior (G), or lateral (H–J) aspect with anterior up. Additional abbreviation: Do, dorsal organ. Scale bars are 200 μm (A–G) and 100 μm (H–J).

The progression of wild type katatrepsis and dorsal closure

The bouncing period is followed by katatrepsis, which usually lasts 2.0 h ($N=24$, $\sigma=0.7$; Movie S1). Katatrepsis involves marked, sustained serosal contraction toward the anterior egg pole. Initial contraction seems to involve a ratcheting up of the serosal window that visibly compresses the embryonic tissue (head and antennae) until resistance to compression causes serosal window rupture due to planar, biaxial tension (Fig. 3, Movie S2). Contraction is significantly faster and farther than normal bounce behavior (Table 1F–G, Fig. 3), although it may follow directly from a bounce minimum (45% of cases, $N=11$). The even faster rate at which the embryo's head drops out following rupture (mean $\pm\sigma$: 11.0 ± 4.2 μm/min, $N=5$) likely reflects the release of hydrostatic compression from the fluid-filled amniotic cavity and the heterogeneous, viscoelastic yolk. The force of release is sufficient to temporarily deform the embryo's head as it presses against the chorion wall (for present purposes, the embryo is a resilient elastic solid). Once the embryo's

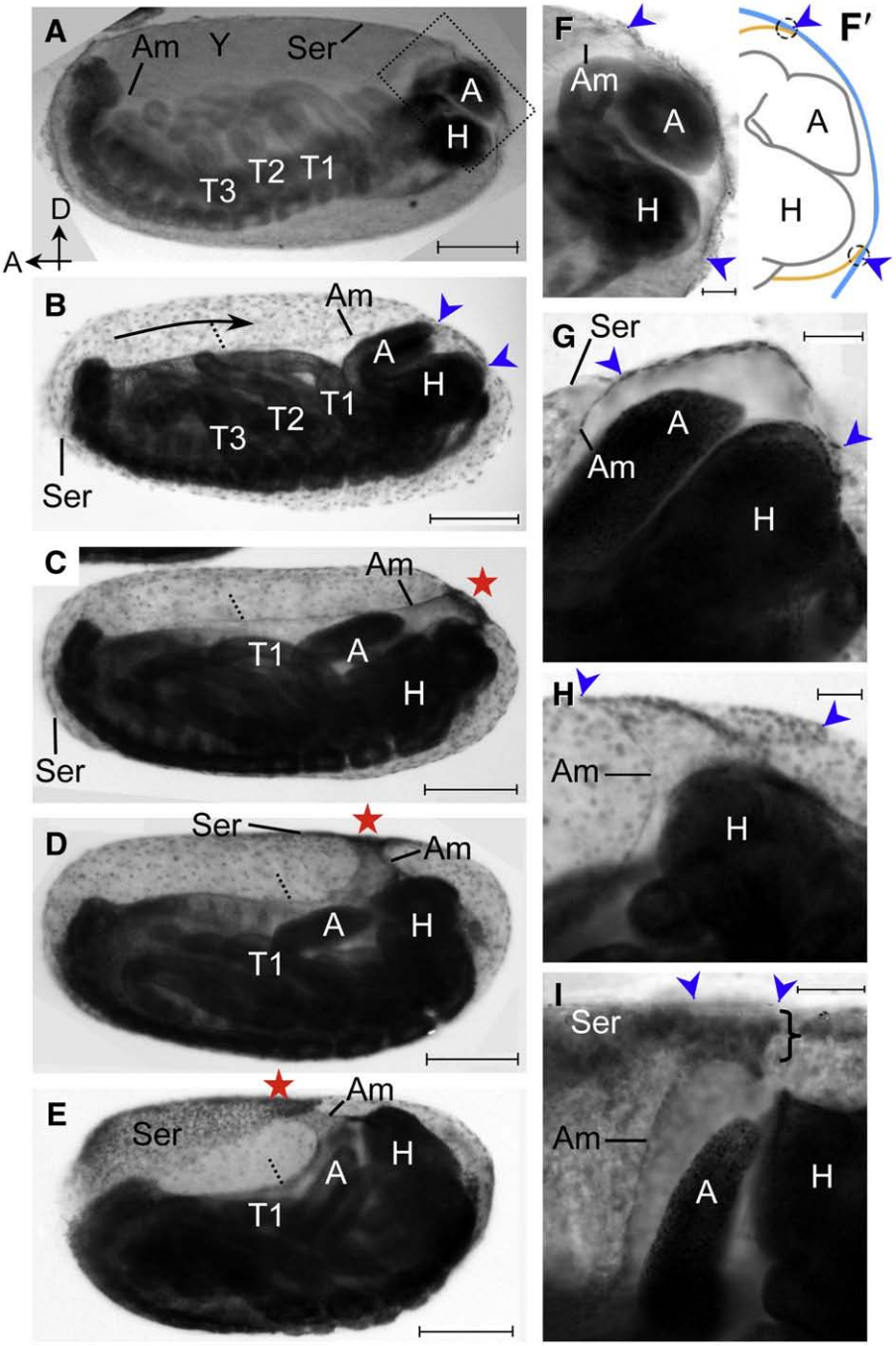

Fig. 5. *Of-zen*^{RNAi} whole mount topography (A–E) and serosal window (F–I) changes, during ectopic serosal contraction. Initially the *zen*^{RNAi} egg is comparable to wild type (A, *cf.* Fig. 2C), but the embryo remains in the egg as body closure progresses (arrow in B, dashed line at leading edge of body closure in B–E), and as the serosa contracts (C–E), pulling the serosal window (position marked by red star) and therefore also the amnion and embryo's head. In images C–E and H–I, the amnion is specifically labeled in the deformed, tube-shaped "amniotic channel" region. Serosal contraction causes deformation of the serosal window (F–I), including thickening (curly bracket in I). The extent of the serosal window – delimited by the point at which the amnion and serosa diverge (*e.g.* black circles in F′) – is marked by blue arrowheads. Image F is of the same egg as in A; images G–I are of different eggs at comparable stages to B–E. Image I is of the same egg as in Fig. 8D, below. Images are in lateral aspect with egg-anterior left and egg-dorsal up. Scale bars are 200 μm (A–E) and 50 μm (F–I).

head has rotated around the posterior pole so that the top points anteriorly, progress of the embryo out of the yolk and toward the anterior pole is relatively rapid as the serosa continues to contract (Fig. 1, Movie S1).

Dorsal closure begins after the embryo has fully emerged from the yolk. It proceeds in a posterior-to-anterior progression (Figs. 4A–D), and is characterized by rhythmic waves that propagate in that direction (Movie S1). In time-lapse movies, waves are visible due to momentary, transverse constriction of dorsal tissue during wave propagation. Waves are associated with final anteriorward progression of the head, and, therefore, further consolidation of the serosal remnant to form the dorsal organ, a discoidal structure (Figs. 4E–F). The dorsal organ forms as the result of a final serosal tissue reorganization whereby it invaginates into the space in the back of the head (Fig. 4H: red arrowhead). The edges of the serosa curl up and over the invaginated tissue, completing the dorsal organ and drawing adjacent amniotic tissue into place over the organ (Figs. 4H–J: blue arrowheads). Ultimately, the dorsal organ degenerates by apoptosis during late dorsal closure (Fig. 4G).

In zen^{RNAi} eggs normal tissue preparation occurs and there is bouncing activity

Oncopeltus zen transcripts are expressed in the serosa from germband stages to the end of the tissue's life, and knockdown of *Of-zen* by RNAi was reported to render the serosa "inert" and unable to effect katatrepsis, leaving the embryo and membranes in the germband stage topography (Panfilio et al., 2006). In light of the above characterization in wild type eggs, at what step do *Of-zen^{RNAi}* eggs fail?

In situ, whole mount visualization of *zen^{RNAi}* eggs reveals that they achieve the tissue reorganization of the normal incipient katatrepsis stage, including germband retraction, appendage folding, amnion smoothing, and even amnion–serosa fusion (Figs. 5A, F, compare to wild type in Figs. 2B′, C; and unpublished observation) (the latter aspect contra Panfilio et al., 2006). However, as previously reported, the embryos then remain in this position as other aspects of post-katatreptic development progress, including darkening of body pigmentation (data not shown, comparable to Figs. 4A–D), and

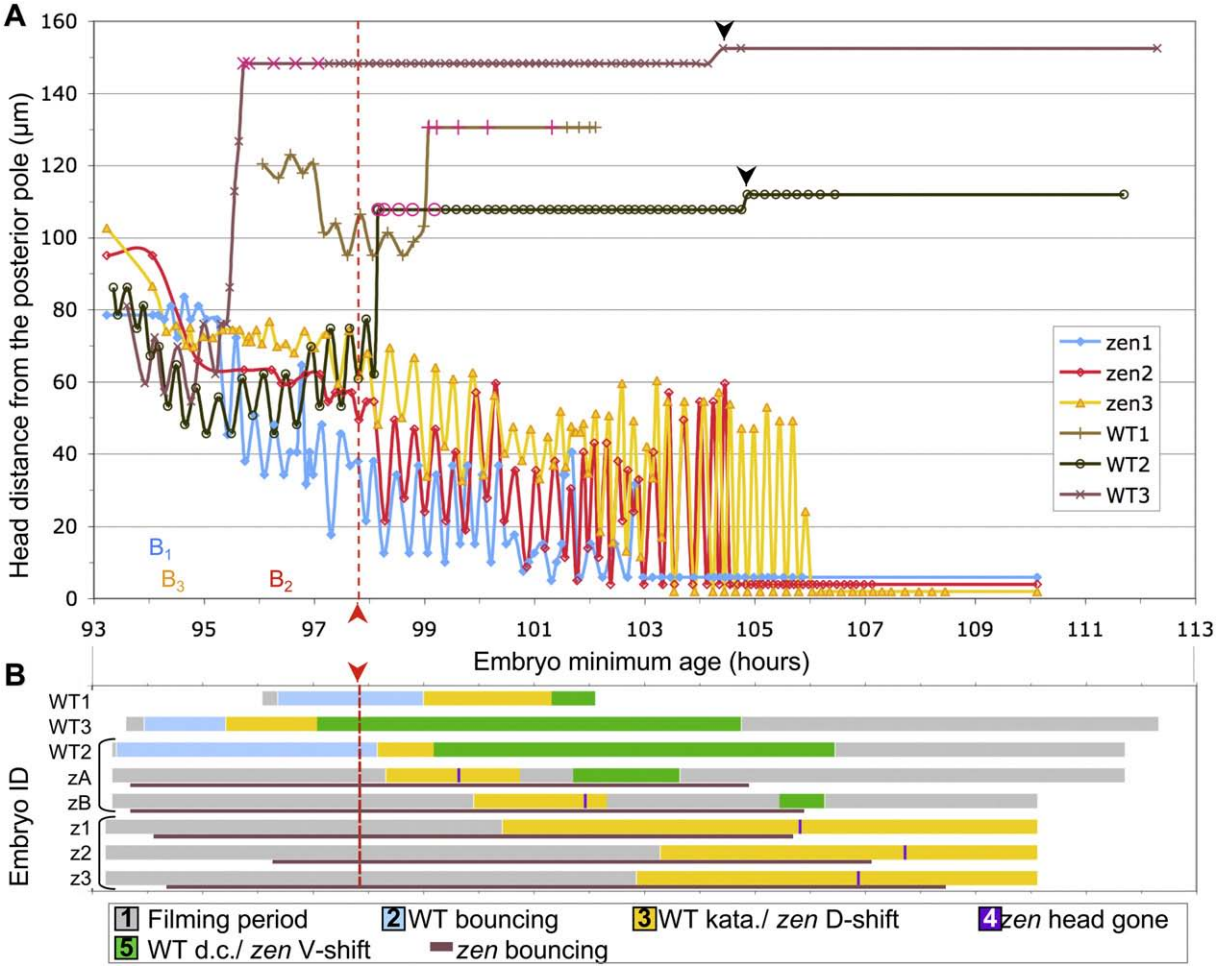

Fig. 6. Comparison of sample *zen^{RNAi}* and WT eggs for timing of activity and occurrence of various events. The dashed red line and red arrowheads indicate the mean time of WT katatrepsis initiation. (A) Distance of the top of the embryo's head from the posterior chorion as a function of time for three WT (brown traces) and three *zen^{RNAi}* (red, yellow, blue traces) embryos at bounce minima and the midpoint between these. For WT embryos, time, but not position, is recorded after the initiation of katatrepsis, indicating katatrepsis stages (pink plot points) and dorsal closure waves (brown points) until the end of filming (final point). Increased distance for two WT traces indicates when the embryo's head fully reached the anterior egg pole (black arrowheads). The onset of bouncing in *zen^{RNAi}* egg *x* is denoted by the position of the notation "B_x"; onset of WT bouncing was not recorded. For all *zen^{RNAi}* embryos, head position was eventually 0 µm, but the traces are staggered for clarity. (B) Occurrence of events for the eggs shown in (A), as well as for those in Movie S3 (WT2, *zen*A, *zen*B), using the same time axis. Plots from eggs filmed together are grouped with brackets. The event "head gone" is when the *zen^{RNAi}* embryo's head and the serosal window are no longer visible laterally. For *zen^{RNAi}* eggs, bouncing activity occurs throughout much of these events (BK bounces and waves during body closure occur in the same direction and cannot be distinguished): duration is indicated by the brown line below the main event line for each egg. Egg-dorsal shift occurred for longer in *zen*1–3 than *zen*A–B eggs, and was not complete by the end of filming for *zen*1–3. Abbreviations: D, dorsal; d.c., dorsal closure; kata., katatrepsis; V, ventral.

embryonic body closure in the correct embryo-posterior to embryo-anterior progression, albeit in the opposite direction to wild type dorsal closure with respect to the egg axes (Figs. 5B–D, and data not shown).

If tissue topography is normal in zen^{RNAi} eggs, what is wrong at the incipient stage that prevents katatrepsis? To quantitatively characterize activity in zen^{RNAi} eggs, time-lapse movies were analyzed from a data set of 4 wild type and 13 zen^{RNAi} eggs recorded for 6–19 h each during the period from incipient katatrepsis through dorsal closure (236 total hours of filming). As wild type and zen^{RNAi} eggs cannot be compared directly by morphology during these stages, they are compared by minimum age after egg laying, with before katatrepsis (BK) and after katatrepsis (AK) ages referring to the average age of katatrepsis initiation at 97.83 h in this data set ($N=4$, $\sigma=1.67$ h).

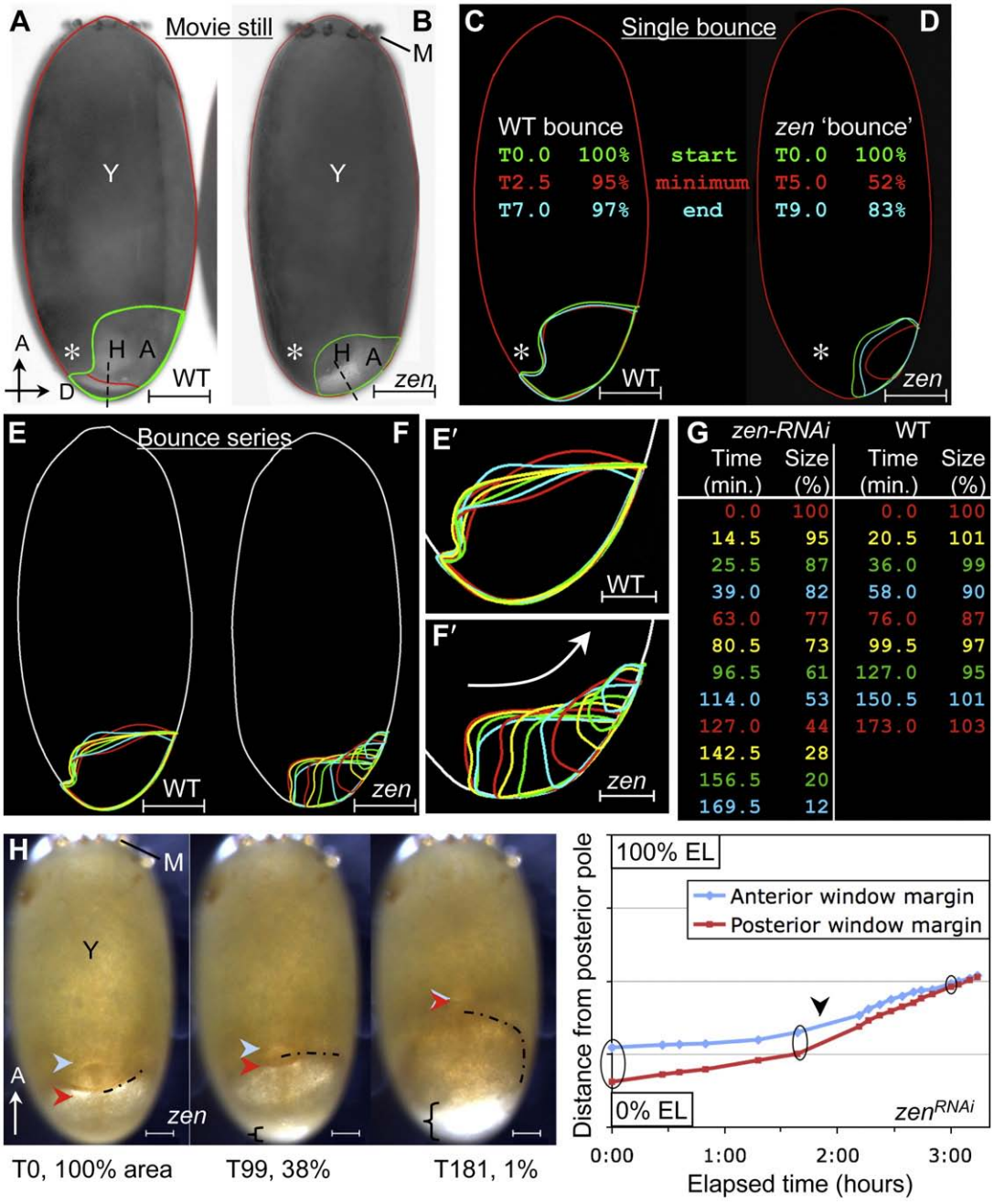

Fig. 7. Comparison of WT and AK zen^{RNAi} bouncing behavior. (BK zen^{RNAi} bounces do not differ substantially from WT; zen^{RNAi} yolk organization is comparable at BK and AK stages [data not shown].) (A–B) Original images with the egg and serosal window outlined. The dashed line indicates the angle of the head. The additional red line in (A) marks the WT serosal window, which is distinct from the chorion, unlike in the zen^{RNAi} egg. The asterisk (also in C–D) marks the yolk in back of the embryo's head. (C–D) Schematics showing the serosal window during phases of one bounce, with the elapsed time in minutes and area of the serosal window (relative to start area) given. (E–F) Schematics showing the serosal window at the end of successive bounces over ~2.85 h, in a WT and zen^{RNAi} egg, respectively. (E′, F′) are respective enlargements, with the arrow in (F′) indicating the direction of shift. (G) Table with elapsed time in minutes (min) and relative window area values for the bounces in (E–F); text colors correspond to the individual outlines in (E–F). (H) Continued anterior shift and shrinkage of the serosal window as it moves over the dorsal egg surface. Below the micrographs, elapsed time in minutes and relative window area are given. The anterior (blue) and posterior (red) margins of the window are plotted as a function of time, relative to total egg length (EL), and are indicated by colored arrowheads in the micrographs. The circled plot points correspond to the micrographs. The top of the embryo's head is partially labeled with a dashed line to indicate how it is pulled forward (*cf.* Figs. 5C–E). In the graph the black arrowhead indicates the approximate time at which the head of the embryo passed a 90° angle. The curly bracket in the second and third micrographs highlights the enlarging space at the posterior egg pole as tissue is pulled anteriorly (*cf.* Figs. 5D–E). All images are oriented with egg-anterior up; egg-dorsal is right in lateral views (A–F); images in (H) are egg-dorsal views. Scale bars are 200 μm (A–F) and 100 μm (E′, F′, H).

The previous classification of the *Of-zen*^{RNAi} phenotype as inert could imply a lack of activity in the incipient katatrepsis egg, yet all observed *zen*^{RNAi} eggs do exhibit a quasi-periodic, bounce-like behavior ($N = 56$; Fig. 6, Movie S3). However, this activity is aberrant in a number of respects. On average, *zen*^{RNAi} eggs begin bouncing 4 h later than wild type, although the strength of this conclusion is limited by a small sample size ($N = 4$ and 7, respectively; Table 1H). Secondly, BK *zen*^{RNAi} eggs have shorter, more frequent bounces than wild type eggs (Table 1I–J), although bounces do not differ significantly in amplitude (distance between bounce minimum and interbounce midpoint; Table 1K). Also of note in BK *zen*^{RNAi} eggs, when at rest between bounces: the embryo's head is less contracted from the posterior pole (Table 1L), the visible portion of the serosal window is smaller (Table 1M), and there is less contraction of the yolk away from the head and antennae (Fig. 7, compare A and B).

After katatrepsis age, *zen*^{RNAi} eggs become even more markedly different from wild type eggs in their behavior. Significant quantitative changes include: increased bounce frequency, a two-fold increase in bounce amplitude and an associated increase in bounce duration, and further reduction in contraction of embryonic tissue from the posterior egg pole (Table 1N–T; Fig. 6). The increased bouncing activity is correlated with qualitative differences: AK *zen*^{RNAi} bounces

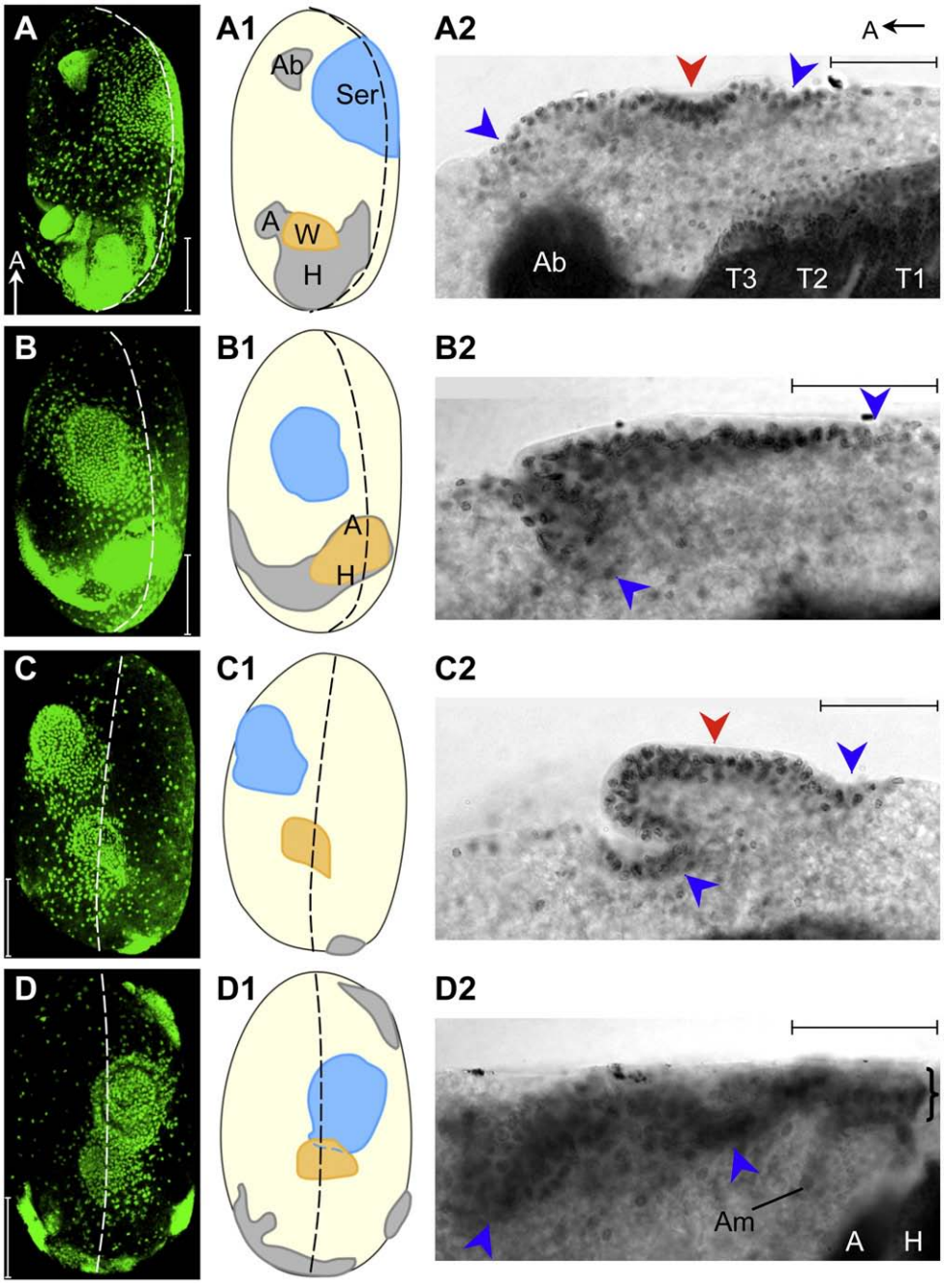

Fig. 8. Progression of *zen*^{RNAi} dorsal organ formation. (A–D) Whole egg micrographs (confocal projections of nuclear stain) in roughly dorsal aspect, with the dashed white line indicating the dorsal midline. (A1–D1) Explanatory schematics: blue, contracted serosa (Ser); orange, serosal window (W); grey, embryonic tissue (A, antenna; Ab, abdomen; H, head); dashed black line, dorsal midline. Due to variability in the site toward which the serosa ectopically contracts, the degree of dissociation of the serosal window and the dorsal organ (= contracted serosa) differs between eggs and does not correlate with the degree of morphological development of the dorsal organ. (A2–D2) Developing dorsal organs in lateral aspect (right side for A2, left side for B2–D2); annotations: blue arrowheads, curling serosal edges (*cf.* Figs. 4H–I); red arrowhead, central invagination (*cf.* Fig. 4H). The embryo shown in (D–D2) is the same as in Fig. 5I. Images are oriented with anterior up (A–D, A1–D1) or left (A2–D2). Scale bars are 250 μm (A–D) and 100 μm (A2–D2).

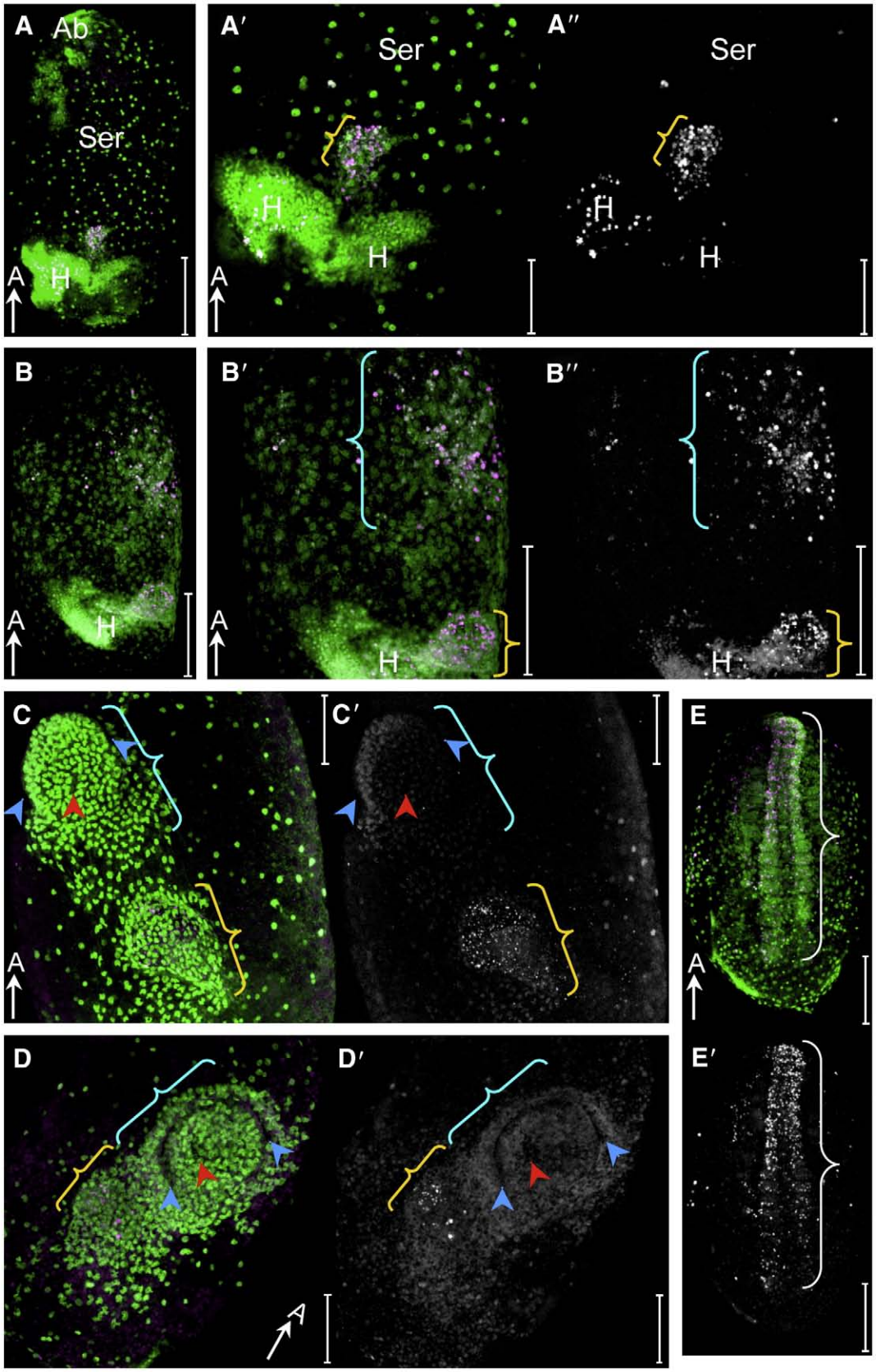

Fig. 9. Patterns of apoptosis in *zen*^{RNAi} eggs (magenta: Caspase-3; green: nuclear counterstain): (A) before serosal tearing, (B) mid serosal contraction, (C–D) advanced serosal contraction and dorsal organ formation, and (E) in embryonic tissue. Images identified by the same letter are of the same embryo. The eggs in (C–D) are the same as in Figs. 8C–D, respectively. Cell death can be seen consistently in the serosal window (A–D) and in embryonic neural tissue of the brain (A) and ventral nerve cord (E, curly white bracket), but only to a limited extent in the contracted portion of the serosa (B, not C–D). Annotations: orange curly bracket, serosal window; blue curly bracket, contracting serosa (*cf.* Figs. 8A1–D1); blue arrowheads, curling serosal edges; red arrowhead, central invagination (*cf.* Figs. 4H–J, 8A2–D2). Views are egg-dorsal (A, C, D), egg-dorsal-left (B), and egg-ventral (E), with egg-anterior up as indicated. Scale bars are 250 μm (A, B–B″, E), 125 μm (C–D′) and 100 μm (A′–A″).

deviate substantially from a simple, anterior–posterior linear movement. Specifically, the angle of movement shifts egg-dorsally from an anterior–posteriorly centered position both within a single bounce (Figs. 7C–D) and over time with successive bounces (Figs. 7E–F). In fact, bounces are better described as contraction and then relaxation of the serosal window perimeter, which in older eggs occurs without any change in embryonic tissue position (Fig. 6A, from 103 h). Within a single bounce, AK zen^{RNAi} eggs' serosal windows may contract to only half the interbounce size, whereas wild type bouncing involves only a small decrease in area (Figs. 7C–D). When wild type bounces are preceded by a contraction, there is an anteriorward shift in position; in contrast the equivalent movement in AK zen^{RNAi} eggs is an overall dilation of the serosal window region (data not shown). Ultimately, with each bounce the serosal window reduces in area and shifts egg-dorsally until it is no longer visible in lateral aspect due to its decreased size — a process that may last 2.74 h ($N=10$, $\sigma=1.42$; Figs. 6B [event 3 to event 4], 7F–G).

The zen^{RNAi} serosa belatedly contracts and forms an ectopic dorsal organ without serosal window rupture

Coupled to the contractility of the serosal window perimeter is contractility of the serosa itself. Far from being inert, the zen^{RNAi} serosa manages to contract anteriorly despite the lack of window rupture (Figs. 5C–E, 8A–D, first two columns), and this is the cause of the egg-dorsal serosal window shift described above (Fig. 7F). Serosal contraction is ectopic and late, with a number of consequences for the serosa, amnion, and embryo.

Normally, the serosa contracts to the anterior egg pole in a relatively symmetric fashion with respect to the dorsal–ventral axis (Fig. 1D), and is only later displaced to the dorsal side by the embryo's head (Fig. 1E). In zen^{RNAi} eggs, the location of the contracted serosa is nearly always ectopic (87%, $N=15$), and most commonly occupies a dorsal-left position in the anterior half of the egg (40%, $N=15$; Fig. 8, first two columns). In these cases, the final resting place of the serosa is over a broad span of one-third EL, from 33 to 77% EL (means, $N=7$). Despite the unusual context, autonomy of late serosal reorganization is such that a rudimentary dorsal organ forms (Fig. 8, third column). The zen^{RNAi} dorsal organ is discrete and has strongly curled edges (compare Figs. 4H–I, 8B–C), although it appears to sink into the yolk with only a limited suggestion of invagination (compare Figs. 4H, 8A, C, 9C–D). Occasionally, apoptosis is observed in the serosa while it is contracting (Fig. 9B), but in contrast to the wild type dorsal organ (Fig. 4G) or other structures in the zen^{RNAi} egg (Figs. 9A–E), formation of the zen^{RNAi} dorsal organ involves very limited detectable cell death (Figs. 9C–D). Thus serosal degeneration either does not involve caspase-dependent apoptosis, or serosal cell apoptosis has a time course that deviates substantially from wild type (it is either very gradual, or rapid and even later than the time when the serosa sinks below the egg surface), as no trace of the serosa remains in later zen^{RNAi} eggs (Panfilio et al., 2006).

In time-lapse movies, zen^{RNAi} serosal contraction is manifest in the aforementioned dorsal shift in serosal window position (Fig. 7F), which continues until the window disappears altogether from the dorsal egg surface at about 50% EL (Fig. 7H). Visible zen^{RNAi} serosal contraction begins much later than wild type katatrepsis, on average starting even slightly later than dorsal closure (Table 1U–V). Despite these peculiar tissue movements, zen^{RNAi} embryos go on to complete dorsal closure at the normal time (Table 1W), indicating either that dorsal closure is initiated at the normal time, or that any delay is compensated for by the fact that everted bodies are smaller and may take less time to close.

In order for the serosa, which formerly occupied the entire egg surface, to contract if the window does not rupture and create an opening, the zen^{RNAi} serosa itself must eventually tear somewhere else. After tearing, the edge of the serosa is initially ill defined (Fig. 8A). Even when the serosal edges are discrete and have curled during dorsal organ formation, there are still a few stray nuclei over the egg surface, distinct from the ever-present subsurface yolk nuclei (Figs. 8B–D). As the site of serosal contraction is variable, it follows that the site at which the serosa tears is also stochastic, though it must initiate on the opposite side of the egg and therefore often in the posterior ventral region.

While the zen^{RNAi} serosa tears to accommodate its own contraction, the fused amnion–serosa border of the serosal window perimeter is firmly maintained (hence the window shift as a consequence of wild type-like amnion–serosa tissue continuity: *cf.* Figs. 1B–E, blue arrowheads, and Figs. 5C–E, red stars). Further, the amnion remains firmly joined to the embryo at its lateral flanks, as ever. Therefore, within the yolk the amnion and the embryo are pulled by the contracting serosa. The pulling force deforms the amnion as it is stretched and attenuated below the egg surface, forming a tubular shape in the region of the amnion below the serosal window (Figs. 5C–E, G–I). Above this 'amniotic channel', the serosal window may become multiple cell layers thick as it compressed (Fig. 5I). Throughout the period of ectopic serosal contraction, even before the serosa tears, there is apoptosis within the serosal window and in the underlying amniotic channel (Figs. 9A–D). Although the unusual mechanical stress exerted by the contracting serosa on the amnion may hasten the process of programmed cell death in the amniotic channel, the two events are independent. There is no correlation between whether the connection to the amnion persists or has already degenerated, on the one hand, and the degree of serosal contraction and dorsal organ formation, on the other (data not shown).

Whole-egg movements in time-lapse movies (Fig. 6B) can be correlated with specific topographical rearrangements and thereby explained. There are two phases to zen^{RNAi} serosal contraction: stepwise during aberrant bouncing (Figs. 6B [prior to event 4], 7F, Movie S3), and then more rapidly via a smooth egg-dorsal rolling of tissue that often involves wholesale tissue contraction away from the posterior egg pole (Figs. 6B [after event 4], 7H, Movies S3–S4). Often the dorsal shift is later reversed during an egg-ventral roll (69% cases, $N=13$; Fig. 6B, event 5). Eventually, the tissues relax to the posterior pole. The transition between step-wise and smoother, faster serosal contraction may correspond to when the serosa tears and thereby lessens resistance to its own contraction. Alternatively, the change in dorsal shift may be due to the embryo, whose head becomes tucked embryo-ventrally during serosal contraction (Fig. 5E). Once the top of the head has passed through an angle >90°, embryonic tissue resistance is largely overcome, as the rate of serosal window shift increases from that point (Fig. 7H plot: 3.5-fold mean rate increase; Movie S4). Additionally, head tucking accounts for the wholesale tissue contraction away from the posterior (Fig. 7H: second and third micrographs; Movie S3). The subsequent ventral tissue shift and loss of posterior tissue contraction (Fig. 6B, Movie S3) likely reflects relaxation of the embryonic tissue (and yolk) as the amnion–serosa connection degenerates and the pulling force of the serosa is abrogated.

Discussion

Wild type Oncopeltus *preparation, katatrepsis, and dorsal closure conform to the hemimetabolan consensus*

Pre-katatrepsis preparation events are shown here by whole mount visualization for the first time (Fig. 2), and comprise: germband retraction, elimination of intervening yolk and amnion-serosa fusion over the head, and appendage folding and amniotic cavity remodeling. This account largely corroborates previous, partial descriptions of hemipterans and other hemimetabolous insects, although with some differences in the occurrence and sequence of these events (Anderson, 1972; Butt, 1949; Cobben, 1968; Dorn, 1976;

Enslee and Riddiford, 1981; Johannsen and Butt, 1941; Kelly and Huebner, 1989; Mahr, 1960; Mellanby, 1936; Wheeler, 1893). Of particular interest are the morphogenesis of mature epithelia during amniotic cavity remodeling and amnion–serosa fusion, which warrant further study.

Time-lapse visualization of the initiation of katatrepsis reveals that it involves serosal contraction until the embryo provides sufficient passive resistance so that biaxial tension on the serosal window causes its rupture (Fig. 3E, Movies S1–S2), similar to observations in the fellow heteropteran *Saldula saltatoria* (Cobben, 1968).

Dorsal closure in a posterior-to-anterior progression is typical of katatreptic species (Fig. 4) (Kelly and Huebner, 1989; Slifer, 1932), in contrast to the simultaneous zippering from the canthi at both ends of the amnioserosa in *Drosophila* (Hutson et al., 2003). This may be due to the location of the serosal remnant, the dorsal organ, in the anterior dorsal region. The orderly contraction of the serosa to form a discoidal structure of high columnar cells (Figs. 4H–I; Butt, 1949; Enslee and Riddiford, 1981; Mellanby, 1936) contrasts with its rapid degeneration once the dorsal organ has formed (Fig 4G).

New insights from time-lapse movies: Pre-katatrepsis bouncing behavior

This study provides the first illustration and quantification of the phenomenon of pre-katatrepsis bouncing behavior (Fig. 3). Bouncing may have been observed in two previous hemimetabolous studies that described various contractions and compressions when the "serosa-yolk system is very active" before katatrepsis (Cobben, 1968). Slifer (1932) attributes such a movement to progressive detachment of the serosa from its cuticle. Although this is a necessary prerequisite to the contraction and sliding of tissue during katatrepsis, its consequences for observable activity are unclear. Cobben (1968) posited serosa/yolk-driven anterior compressions of the amniotic cavity fluid that bulge the posterior amnion and bring it into contact with the serosa, perhaps aiding in serosal window formation. Quantification of bounce behavior in *Oncopeltus* also implicates an egg-anterior pushing force followed by relaxation, as the posterior bounce phase is greater than the anteriorward phase (Table 1A–C). However, given that bounces are greater when preceded by an anteriorward contraction (Table 1D–E), the impetus cannot solely consist of a pushing force. During a bounce, the embryo and the extraembryonic tissue of the serosal window move at slightly different rates and are not always in contact (data not shown), which likely precludes pushing by the embryo as the motive force but does not elucidate whether it is due to the agency of the serosa, amnion, or yolk system. Alternatively, as a pulsatile force, bouncing may play a role in stress-softening of the serosal window that makes it thinner and increases its relative surface area over the serosal sack, ensuring that it is the site of rupture at katatrepsis initiation.

Although a full biomechanical model of bouncing and the initiation of katatrepsis requires further research, this study provides a foundation, including qualitative description, kinematic analyses, and a preliminary assessment of relevant forces and mechanical properties of the egg (as outlined in Koehl, 1990).

zen^{RNAi} eggs may miss a window of opportunity and lack baseline compression

Irrespective of the exact cause and function of bouncing, it is integral to the comparison of wild type and zen^{RNAi} eggs. The time-lapse data belie the previous interpretation that the zen^{RNAi}-induced failure of katatrepsis results from an "inert" state because zen^{RNAi} eggs do bounce over an extended period and then go on to complete other movements associated with ectopic serosal contraction (Figs. 7–8, Movies S3–S4). These activities were previously unknown because: the former is subtle and could not have been determined from examination of fixed material; and the latter occurs much later than related wild type events (Table 1U), with gross morphological changes (Fig. 8) that are rapid and variable in timing ($N = 11$, mean duration $\pm \sigma$: 4.2 ± 2.7 h, commencing within an >8 hour window), and the end stage phenotype leaves no trace of the final location of these tissues. The time-lapse data reveal two telling defects in zen^{RNAi} eggs at the incipient stage, even while the visualization of fixed tissue topography does not reveal any marked deviations from wild type (Figs. 5A, F).

The distinction of before and after katatrepsis age (BK and AK) reveals changes in zen^{RNAi} bouncing over time. At BK ages, bouncing may start later in zen^{RNAi} eggs and then is more frequent and of shorter duration when it does (Table 1H–J). When the age for katatrepsis has passed (AK) and the zen^{RNAi} eggs remain in the pre-katatrepsis position, bouncing becomes even more energetic and aberrant (Figs. 6–7, Table 1N–Q). This is suggestive of a physiological stress response: it is comparable to exaggerated constriction–dilation activity at the amnion–serosa border (= former serosal window perimeter) in wild type eggs that attempt to complete katatrepsis under conditions of anoxic stress (data not shown). Collectively, these data suggest that there is a temporal window of opportunity in which to initiate katatrepsis, and that subsequent tissue behavior indicates when this physiologically or mechanically favorable period has been missed in zen^{RNAi} eggs. This indicative behavior is evident even before the zen^{RNAi} serosa belatedly contracts. The fact that the rate at which events proceed is not slower (the delay in zen^{RNAi} activity does not worsen over time, Table 1H, U) further supports the occurrence of a discrete delay that is specific to the incipient katatrepsis period. Previous experimental studies that generated everted embryos also found evidence for "a critical period for performing katatrepsis" (Ando, 1955), after which serosal contraction was incapable of effectively causing window rupture or pulling of the embryo (Truckenbrodt, 1979).

The second problem concerns pressure within the egg. Based on the serosal expression of *Of-zen* and the failure of katatrepsis after *zen* knockdown, it was already inferred that *Of-zen* has a contractile role (Panfilio et al., 2006). The data presented here clarify one aspect of this role. Strong, sustained contraction ('Phase II') is required for extraembryonic membrane rupture and the progression of katatrepsis (Fig. 3A, Movies S1–S2). However, this strong contraction is preceded, in wild type, by an extended period during which the serosal sack is specifically contracted away from the posterior egg pole (Figs. 1F–F′, 3A–B, 7A). This baseline level of contraction ('Phase I') is achieved gradually over a number of hours and is then *sustained*, before the onset of bouncing behavior and about half a day before the initiation of katatrepsis (Fig. S1). In cricket eggs, baseline contraction initiates and then is sustained *days* before Phase II contraction commences (Mahr, 1960). In *Oncopeltus* BK zen^{RNAi} eggs, the lack or loss of contraction from the posterior pole (Fig. 6A [prior to B_2 and B_3], Table 1L) may indicate an inability to generate or sustain sufficient preparatory (Phase I) contractile force over the entire serosa and its contents. As wild type serosal window rupture (Phase II) involves compressive stress on the serosal sack to generate tensile stress on the window, it may require Phase I compression as a starting point, which is not the case in zen^{RNAi} eggs at katatrepsis age. Furthermore, in AK zen^{RNAi} eggs, the limited Phase I contraction is lost (Fig. 6A [from 103 h], Table 1R–T), even as aberrant bounce movements increase and herald ectopic serosal contraction (the zen^{RNAi} equivalent of Phase II contraction). Thus Phases I and II seem to be temporally and mechanistically distinct. One possibility is that whereas Phase II contraction is clearly accomplished by the serosa, Phase I contraction may be mediated by the yolk, consistent with previous observations of autonomous activity by this substance (Cobben, 1968; Mahr, 1960; Sander, 1959; Sander, 1967; Truckenbrodt, 1973; Truckenbrodt, 1979; Vollmar, 1972). If so, this would imply a role for *zen* and the serosa in regulating yolk reorganization.

The serosal window: The key structure for epithelial rupture, and the time course of its creation

zen^{RNAi} eggs successfully form the serosal window by fusion of the amnion and serosa over the embryo's head. The strength of amnion–serosa fusion is evident in the subsequent capacity of the serosa to pull the amnion and embryo via this attachment site when it contracts ectopically. Furthermore, the serosa is, to an extent, capable of anteriorward contraction and dorsal organ formation. Despite this, katatrepsis completely fails in *zen*^{RNAi} eggs because the serosal window never ruptures and therefore the embryo remains within the amnion and yolk. Therefore, the knockdown of *zen* causes a loss of competence to effect rupture of this tissue. Understanding the initiation of katatrepsis and the *zen*^{RNAi} phenotype now hinges on the question: how is a controlled hole created? What are the properties of the serosal window that cause it to tear in the middle while the border remains firm? The lack of pressure due to the *zen*^{RNAi} deficient baseline contraction of the system (Phase I, discussed above) could account for the failure of rupture if the window is never mechanically challenged, as could the shorter BK bouncing period, if bouncing does aid in mechanical preparation. However, other data suggest that the serosal window itself is also improperly prepared.

Even before it actively shrinks, the BK age *zen*^{RNAi} serosal window is significantly smaller than the wild type window (Table 1M, beginning of Movie S3). Faulty early preparation events may be responsible for the small window. In wild type, following Phase I baseline contraction, there is a yolk-embryo reorganization within the serosal sack that specifically involves the marked anteriorward withdrawal of the yolk behind/ventral to the embryo's head, and the concomitant posterior-ventral rotation of the embryo's head and the serosal window so that they are centered over the posterior pole (Figs. 7A, C, Fig. S1, beginning of Movies S1, S3 [left egg]; Mahr, 1960). In *zen*^{RNAi} eggs the position of the ventral-posterior yolk and the angle of the embryo's head are comparable to that of wild type eggs at germband stages prior to this reorganization (compare Fig. S1A–C with Figs. 7B, D and beginning of Movie S3 [middle and right eggs]). The retention of a dorsalward curvature of the embryo's head and a dorsally biased position of the serosal window could predispose the system to shifting in a dorsal direction, and thus account for the direction and final site of ectopic serosal contraction. As Phase I contraction and yolk-embryo reorganization at the posterior pole precede bouncing activity (Fig. S1), insufficient execution of these early events could also account for the observed delay in activity – for missing the temporal window of opportunity – discussed above.

In sum, events that occur hours before katatrepsis are necessary both for baseline contraction (Phase I, discussed above) and for subtle reorganization of the yolk and embryo at the posterior pole that may (a) increase the surface area of amnion–serosa contact to form the serosal window, and/or (b) ensure the site of maximum stress is centered on the window at the time of Phase II contraction. Even if the size of the window is large enough in terms of number of cells involved, tension generated by rotation of the head and the stretching of the window may be necessary to ensure that it is weak enough to rupture. One alternative possibility these data do not address is that preparation for katatrepsis involves local, active weakening of tissue integrity within the serosal window – *e.g.*, loss of cell–cell adhesion or degradation of the extracellular matrix – in which case *zen* could have a specific role in the alteration of intercellular structural integrity. It is also unknown how the window is determined (how, and how many, amniotic and serosal cells are recruited). Nonetheless, wild type-like attachment of the epithelia at the serosal window perimeter (= amnion-serosa border) was demonstrated (Fig. 5) and other investigations reveal no difference between wild type and *zen*^{RNAi} eggs with respect to the nature of fusion within the 'pane' of the serosal window (unpublished observation), and thus I favor a biomechanical explanation for the failure of rupture.

Detailed characterization of katatrepsis or membrane uncovering is germane to studying the role of *zen* in insects spanning the polyneopterous, paraneopteran, and holometabolan lineages (Panfilio et al., 2006; van der Zee et al., 2005; K. Panfilio, T. Nakamura, T. Mito, S. Noji, unpublished observation). What do the defects in the *Oncopeltus zen*^{RNAi} egg, as interpreted here, mean for understanding the role of this gene? RNA interference of *Of-zen* does not impair amnion-serosa fusion to form the serosal window, but the subsequent step of window rupture does not occur. These findings contrast with the failure of amnion-serosa fusion after knockdown of *Tc-zen2* in the beetle *T. castaneum* (van der Zee et al., 2005), and suggest that, despite a common end stage phenotype of embryonic eversion after RNAi for *Tc-zen2* and *Of-zen*, these genes have different specific functions in effecting late extraembryonic morphogenetic movements.

Of-zen is specifically expressed in extraembryonic tissue as opposed to the yolk or embryo, and in particular this expression persists throughout the serosa and throughout germband, katatrepsis, and dorsal closure stages (Panfilio et al., 2006). Therefore any relevant reorganization of yolk and embryo (serosal sack contents) is likely mediated by whole egg reorganizational events driven, or coordinated by, the serosa, even if they are most readily – or even primarily – observed at the posterior egg pole. The defects of a missed temporal window of opportunity, reduced baseline contraction, and a small, dorsally-angled serosal window all have explanatory power in accounting for the phenomena documented here and for the *zen*^{RNAi} failure of katatrepsis itself. In turn, problems in specific, early reorganizational events that occur hours before katatrepsis could account for these three defects. Although RNAi-mediated knockdown of *Of-zen* completely blocks katatrepsis and yields an all-or-nothing phenotype (Panfilio et al., 2006), nonetheless there seems to be no one point of failure. The role of *Of-zen* is in an array of whole-egg preparatory events rather than in the prominent, discrete Phase II contraction of the serosa and the tissue's own final reorganization into the dorsal organ. This is consistent with the recent hypothesis that "quantitative methodologies" reveal "more subtle genetic effects acting over a broader window of development" than is normally considered (Cooper and Albertson, 2008). Perhaps given the nature of katatrepsis as a large morphogenetic movement it should be unsurprising that understanding the system and its failure involve a whole egg topographical and biomechanical approach.

Acknowledgments

I thank Giselle Walker for assistance with semithin sectioning; Franz Kainz for the gift of *DsRed* double stranded RNA; Cassandra Extavour for the introduction to time-lapse recording; Michael Akam and Evelyn Schwager for helpful discussions during the course of this work; Siegfried Roth, Martina Rembold, Jeremy Lynch, Maria Leptin, and an anonymous referee for useful comments on the manuscript. This work was supported financially by an HHMI Predoctoral Fellowship and then by an Alexander von Humboldt Postdoctoral Research Fellowship to K.A.P., and BBSRC grant BBS/B/07519 to M. Akam.

Appendix A. Supplementary data

Supplementary data associated with this article can be found, in the online version, at doi:10.1016/j.ydbio.2009.06.036.

References

Anderson, D.T., 1972. The development of hemimetabolous insects. In: Counce, S.J., Waddington, C.H. (Eds.), Developmental Systems: Insects, Vol. 1. Academic Press, London, pp. 95–163.

Ando, H., 1955. Everted embryos of dragonflies produced by ligation. Sci. Rep. Tokyo Kyoiku Daig. Sect. B 8, 65–74.

Butt, F.H., 1949. Embryology of the Milkweed Bug, *Oncopeltus fasciatus* (Hemiptera). Agriculture Experiment Station, Cornell University.

Cobben, R.H., 1968. Evolutionary Trends in the Heteroptera, Part I. Eggs, Architecture of the Shell, Gross Embryology and Eclosion. Centre for Agricultural Publishing and Documentation, Wageningen.
Cooper, W.J., Albertson, R.C., 2008. Quantification and variation in experimental studies of morphogenesis. Dev. Biol. 321, 295–302.
Dorn, A., 1976. Ultrastructure of embryonic envelopes and integument of *Oncopeltus fasciatus* Dallas (Insecta, Heteroptera) I. Chorion, amnion, serosa, integument. Zoomorphologie 85, 111–131.
Enslee, E.C., Riddiford, L.M., 1981. Blastokinesis in embryos of the bug, *Pyrrhocoris apterus*. A light and electron microscopic study 1. Normal blastokinesis. J. Embryol. Exp. Morph. 61, 35–49.
Erezyilmaz, D.F., Riddiford, L.M., Truman, J.W., 2004. Juvenile hormone acts at embryonic molts and induces the nymphal cuticle in the direct-developing cricket. Dev. Genes Evol. 214, 313–323.
Glauert, A.M., 1975. Fixation, Dehydration and Embedding of Biological Specimens. Elsevier North-Holland Biomedical Press, Amsterdam.
Handel, K., Grünfelder, C.G., Roth, S., Sander, K., 2000. *Tribolium* embryogenesis: a SEM study of cell shapes and movements from blastoderm to serosal closure. Dev. Genes Evol. 210, 167–179.
Hutson, M.S., Tokutake, Y., Chang, M.S., Bloor, J.W., Venakides, S., Kiehart, D.P., Edwards, G.S., 2003. Forces for morphogenesis investigated with laser microsurgery and quantitative modeling. Science 300, 145–149.
Johannsen, O.A., Butt, F.H., 1941. Embryology of Insects and Myriapods. McGraw-Hill Book Company, Inc., New York.
Kelly, G.M., Huebner, E., 1989. Embryonic development of the hemipteran insect *Rhodnius prolixus*. J. Morph. 199, 175–196.
Koehl, M.A.R., 1990. Biomechanical approaches to morphogenesis. Semin. Dev. Biol. 1, 367–378.
Liu, P.Z., Kaufman, T.C., 2004. *hunchback* is required for suppression of abdominal identity, and for proper germband growth and segmentation in the intermediate germband insect *Oncopeltus fasciatus*. Development 131, 1515–1527.
Mahr, E., 1960. Normale Entwicklung, Pseudofurchung und die Bedeutung des Furchungszentrums im Ei des Heimchens (*Gryllus domesticus*). Z. Morph. Ökol. Tiere 49, 263–311.
Mellanby, H., 1936. The later embryology of *Rhodnius prolixus*. Q. J. Microsc. Sci. 79, 1–42.
Mori, H., 1975. Everted embryos obtained after cauterization of eggs of the waterstrider, *Gerris paludum insularis* Motschulsky. Annot. Zool. Japon. 48, 252–261.
Novák, V.J.A., 1969. Morphogenetic analysis of the effects of juvenile hormone analogues and other morphogenetically active substances on embryos of *Schistocerca gregaria* (Forskål). J. Embryol. Exp. Morph. 21, 1–21.
Panfilio, K.A., 2008. Extraembryonic development in insects and the acrobatics of blastokinesis. Dev. Biol. 313, 471–491.
Panfilio, K.A., Liu, P.Z., Akam, M., Kaufman, T.C., 2006. *Oncopeltus fasciatus zen* is essential for serosal tissue function in katatrepsis. Dev. Biol. 292, 226–243.
Sander, K., 1959. Analyse des ooplasmatischen Reaktionssytems von *Euscelis plebejus* Fall. (Cicadina) durch Isolieren und Kombinieren von Keimteilen I. Die Differenzierungsleistungen vorderer und hinterer Eiteile. Roux' Arch. Entwickmech. 151, 430–497.
Sander, K., 1960. Analyse des ooplasmatischen Reaktionssystems von *Euscelis plebejus* Fall (Cicadina) durch Isolieren und Kombinieren von Keimteilen. II. Die Differenzierungsleistungen nach Verlangern von Hinterpolmaterial. Roux' Arch. Entwickmech. 151, 660–707.
Sander, K., 1967. Mechanismen der Keimeseinrollung (Anatrepsis) im Insekten-Ei. Zool. Anz. Suppl. 31, 81–89.
Schwalm, F.E., 1988. Insect Morphogenesis. Karger, Basel.
Slifer, E.H., 1932. Insect development. III. Blastokinesis in the living grasshopper egg. Biol. Zbl. 52, 223–229.
Truckenbrodt, W., 1973. Über die Entstehung der Serosa im besamten und im unbesamten Ei von *Odontotermes badius* Hav. (Insecta, Isoptera). Z. Morph. Tiere 76, 193–208.
Truckenbrodt, W., 1979. The embryonic covers during blastokinesis and dorsal closure of the normal and of the actinomycin D treated egg of *Odontotermes badius* (Hav.) (Insecta, Isoptera). Zool. Jb. Anat. Ont. 101, 7–18.
van der Zee, M., Berns, N., Roth, S., 2005. Distinct functions of the *Tribolium zerknüllt* genes in serosa specification and dorsal closure. Curr. Biol. 15, 624–636.
Vollmar, H., 1972. Die Einrollbewegung (Anatrepsis) des Keimstreifs im Ei von *Acheta domesticus* (Orthopteroidea, Gryllidae). Roux' Arch. Entwickmech. Organ. 170, 135–151.
Wakimoto, B.T., Turner, F.R., Kaufman, T.C., 1984. Defects in embryogenesis in mutants associated with the Antennapedia complex of *Drosophila melanogaster*. Dev. Biol. 102, 147–172.
Wheeler, W.M., 1893. A contribution to insect embryology. J. Morph. 8, 1–160.
Wigand, B., Bucher, G., Klingler, M., 1998. A simple whole mount technique for looking at *Tribolium* embryos. Tribolium Information Bulletin 38, 281–283.